Portable glucose detector based on nickel oxide modified Screen Printed Carbon Electrode (SPCE)

Fenika Annisa[1], *Djati* Handoko[1,*], *Auliya'u* Darojatin[1], *Annisa Sonya* Puspita[1], *Fitria Yunita* Dewi[1], *Prawitno* Prajitno[1], *Muhammad Hanif* Fajari[2], *Harry Kasuma* Aliwarga[3], and *Tribidasari Anggraningrum* Ivandini [2]

[1]Department of Physics, Faculty of Mathematics and Natural Sciences (FMIPA), Universitas Indonesia, Depok 16424, Indonesia
[2]Department of Chemistry, Faculty of Mathematics and Natural Sciences (FMIPA), Universitas Indonesia, Depok 16424, Indonesia
[3]UMG IdeaLab, South Jakarta 12930, Indonesia

Abstract. A portable and low-cost system prototype for glucose detector based on LMP91000EV M potentiostat has been created. Characterization of Screen-Printed Carbon Electrodes (SPCE) without modification (bare SPCE) and modified nickel oxide (NiO/SPCE) was carried out with a commercial potentiostat to see the effect of nickel oxide in detecting glucose. Through the electrochemical impedance spectroscopy method, the Rct value of 1,276.79 Ω is obtained for NiO/SPCE and 429.06 Ω for bare SPCE, so that NiO/SPCE has a slower electron transfer rate. Meanwhile, through the cyclic voltammetry method, the surface-active electrode area is 7.1×10^{-2} cm^2 for NiO/SPCE and 6.9×10^{-2} cm^2 for bare SPCE, so that NiO/SPCE is more sensitive in detecting glucose. When the glucose concentration is varied, the Limit of Detection (LOD) and Limit of Quantitation (LOQ) values of NiO/SPCE are smaller, specifically 1.807 mM and 6.024 mM than bare SPCE, specifically 2.629 mM and 8.762 mM, so NiO/SPCE is more sensitive. When the scan rate is varied, the gradient value of NiO/SPCE is smaller, specifically -8.14×10^{-4} mA s/mV than bare SPCE, specifically -9.62×10^{-4} mA s/mV, so NiO/SPCE is not more sensitive. Next, comparing a prototype system that Trans Impedance Amplifier (TIA) gain is varied and a commercial potentiostat. As a result, the cyclic voltammogram per cycle on commercial potentiostat is more stable. The smaller the TIA gain on the system prototype, the more stable it is, this is because the noise that is amplified is getting smaller.

Keywords. Cyclic voltammetry, electrochemical impedance spectroscopy, glucose, nickel oxide, screen printed electrode

* Corresponding author: djati.handoko@ui.ac.id

1 Introduction

In 2021, Indonesia ranked 5th in the world with the most diabetes mellitus patients [1]. Diabetes mellitus is indicated by increased blood sugar or glucose levels [2]. Normally, blood sugar in human body is about 5 mM [3]. A popular, low-cost, and widely produced electrochemical sensor is the screen-printed carbon electrode [4] used to detect glucose. The electrode material can be modified, nickel oxide was chosen because it is designed to be an electrocatalyst in the electrochemical oxidation of small organic molecules [5] and nickel is sensitive to glucose [6]. Generally, electrochemical sensors have three electrode configurations, namely working electrode (WE) as the electrode where the reaction to the analyte being measured occurs, reference electrode (RE) as a standard and stable potential source compared to WE [7], and counter electrode (CE) as an electrode that ensures that current does not flow into the RE so that it does not interfere with the potential in the RE [8]. The effect of the modified nickel oxide on the screen-printed carbon electrode in detecting the sample, so that the bare SPCE and NiO/SPCE sensors were compared to analyze the ability of nickel oxide to detect glucose.

Electrochemical analysis methods are used to analyze the detection results with electrochemical sensors, for example there is a cyclic voltammetry (CV) that investigates the oxidation reduction process [9], the graph is called a cyclic voltammogram which has a characteristic duck-like shape. The characteristics of the observed voltammogram are the peak current height (IP) and the peak current potential (EP) for quality control and verifying that something printed on the electrode screen is in accordance with the expected output [4]. The effect of variations in the scanning rate and glucose concentration on the sensor is analyzed using the cyclic voltammetry method. Another example is electrochemical impedance spectroscopy (EIS), which used to analyze the interface properties of the electrode surface [10]. The results of EIS detection are Nyquist plots for electrode characterization based on the value of charge-transfer resistance (Rct), which is a semicircle diameter [11].

The data acquisition system to process glucose detection results needs to be equipped with a device capable of inputting signals and voltages from the oxidation-reduction reaction, namely a potentiostat [12]. A system prototype has been made which is generally open source, low cost, and portable based on potentiostat module LMP91000EVM, in contrast to commercial systems which are expensive and have a large size that makes them difficult to carry. Therefore, the performance of the system prototype is compared with the potential of a commercial potentiostat.

2 Materials and method

2.1 Sample preparation

D(+)-glucose anhydrous from Merck, sodium hydroxide (NaOH), monopotassium phosphate (KH_2PO_4) and dipotassium phosphate (K_2HPO_4) from Merck as ingredients for generating PBS (Phosphate-Buffered Saline), potassium ferricyanide ($K_3[Fe(CN)_6]$) from Smart Lab, and aquadest as solvent are the materials required for the production of samples in this research. The following samples were made: (1) $K_3[Fe(CN)_6]$ 0.1 M dissolved in 0.1 M PBS pH 7.4 and (2) D(+)-Glucose (1 mM, 3 mM, 5 mM, 7 mM, and 9 mM) in 0.1 M NaOH solution. Each sample was taken as much as 20 µL using a micropipette to be tested on the sensor surface.

2.2 System prototype

The prototype glucose detection system is shown in Fig. 1, consisting of an electrochemical sensor, an LMP91000EVM, a Raspberry Pi, and a GUI display device. The electrochemical sensor is in the form of a screen-printed carbon electrode for detecting electrochemical reactions on glucose modified by nickel oxide (NiO/SPCE) [5] and unmodified (bare SPCE) [13] from Dropsens. Then, the sensor is connected to the LMP91000EVM [14] from Texas Instrument via the connector from iorodeoo. The LMP91000EVM acts as a potentiostat that drives analog front-end sensor operation and performance for electrochemical sensors. Next, the LMP91000EVM is connected to the Raspberry Pi 3 model B+ [15] which will process the CV sweep data from the LMP91000EVM based on the output voltage generated. This Raspberry Pi is given a voltage source that comes from a power bank of 5 V, the use of a power bank aims to minimize voltage changes. The Raspberry Pi is also connected to the monitor as a GUI viewer via an HDMI cable, or wirelessly to a laptop or smartphone via the VNC viewer application, as shown in Fig. 2.

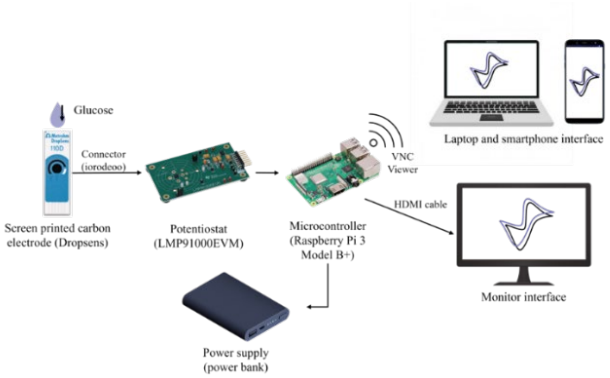

Fig. 1. Glucose detector portable system design.

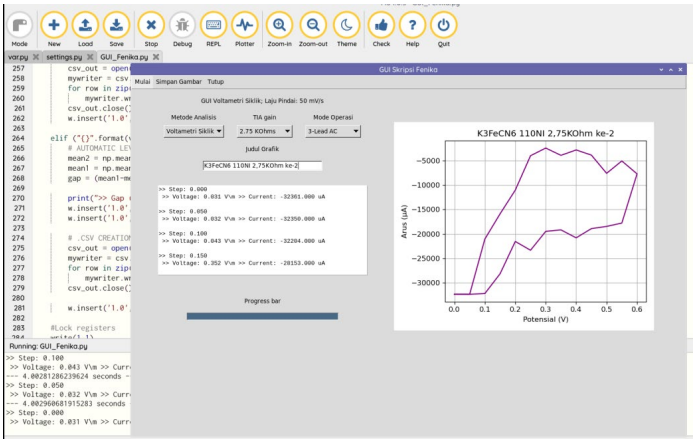

Fig. 2. The system GUI displays a cyclic voltammogram via the VNC viewer application.

The CV sweep process is carried out based on steps starting from 0 % to 24 % originating from the division of the bias variable on the VREF reference voltage source of 2.5 V configured by the reference control register (REFCN). Then, the voltage is amplified by the control amplifier (A1) and provides zero internal voltage and bias from RE, whose output

goes to CE. The current detected by WE will be low-pass filtered by RLOAD and output capacitance. After that, it is amplified in the transimpedance amplifier (TIA), so that the current generated by the sensor becomes a voltage with a TIA gain of the same value as RTIA. The bias cell and TIA on the LMP91000 can be adjusted and programmed via the I2C interface. Pull-up resistors or current sources are required on the SCL and SDA pins to set HIGH and, when not required, LOW [16]. The output voltage is processed on the Raspberry Pi and then into the voltage and current values that make up the cyclic voltammogram shown in Equation (1) and Equation (2):

$$V = (V_{RAW} \cdot V_{MAX})/binmax + V_{REF}\ (V) \quad (1)$$

$$I = (V - (V_{REF}/2))/R_{TIA} \cdot 10^6\ (\mu A) \quad (2)$$

where V is the processed voltage, V_{RAW} is the raw output voltage read by the ADC, V_{MAX} is the full scale voltage range obtained from $V_A - (V_{REF}/2^{16})$ with V_A as the analog supply (5 V), binmax is the maximum decimal value for an n-bit binary code limited to 16-bit, $2^{16} - 1 = 65{,}635$, VREF is the reference potential for the desired sweep (2.5 V), I is the current obtained, and R_{TIA} is the gain resistance of the TIA selected [17]. Figure 3 shows a schematic of the LMP91000 in 3-lead operating mode in which three electrodes are used for measurement.

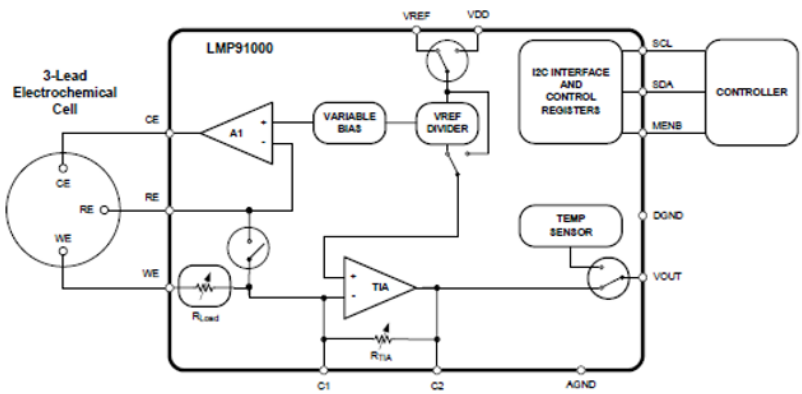

Fig. 3. Schematic of the LMP91000 in 3-lead operating mode.

The three programs that have been made are first "var", which contains variables, register addresses, and I2C and SPI communication configuration parameters required, second "settings", which contains function definitions that will be used in "GUI_Fenika", such as processing data from an ADC, and last "GUI_Fenika", which contains commands to display and manage the GUI from tkinter. The first step is to run the program "GUI_Fenika". The GUI appears and the green LED lights up. Insert the sensor you want to test (bare SPCE or NiO/SPCE) into the adapter and drop the sample you want to test (glucose or potassium ferricyanide) onto the electrode surface. Sets the combo box analysis method, TIA gain, and operation mode. This experiment chose the "cyclic voltammetry" analysis method, the gain of TIA with variations of 2.75 Ω, 3.5 Ω, and 7 Ω, and the operating mode "3-LEAD AC" because the sensor used has three electrodes. Then, enter the title of the graph as the name of the .csv file containing the current and voltage data and the .png file containing the cyclic voltammogram image in a folder named "tool CV data". The voltage sweep process starts after pressing "*mulai*" (start) on the menu bar. The green LED will turn off and the red LED

will light up, indicating the sweep process is in progress. The progress bar will run, showing the progress of the data retrieval process. Current and voltage data along with a cyclic voltammogram graph can be seen in real time. After the data retrieval process is complete, the red LED turns off, the green LED lights up, the progress bar will return to the beginning, and the csv file containing current and voltage data is automatically saved. If you want to save the cyclic voltammogram image in the form of a png file, press "*simpan gambar*" (save image) on the menu bar. Then, repeat the experiment for sample variation, sensor, and TIA gain. If you have not done the test, you can press "*tutup*" (close) to close the GUI. The green LED will automatically turn off. The data collection process is also represented through the flow chart in Fig. 4.

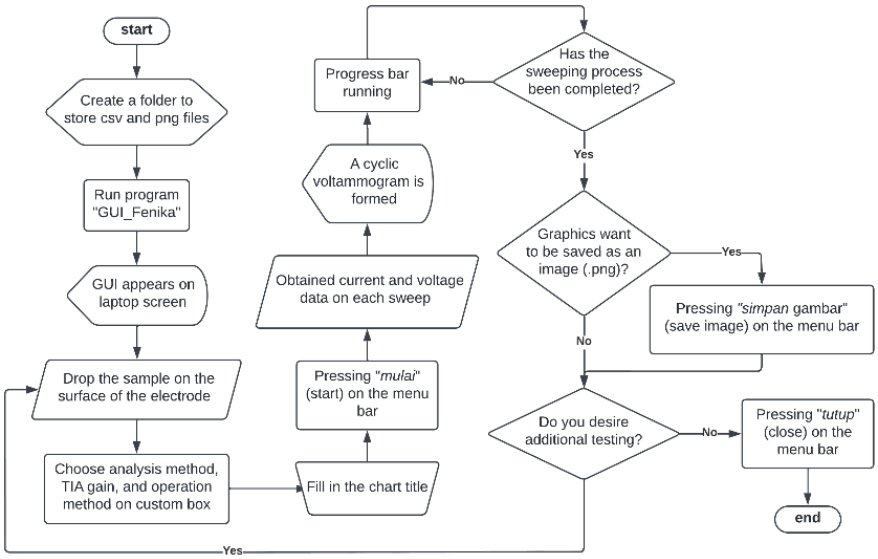

Fig. 4. Data retrieval flowchart utilizing a system prototype.

3 Results

3.1 Electrode characterization

Electrode characterization was carried out using a commercial potentiostat. The Nyquist plot generated by the EIS method to analyze the interface of the bare SPCE and NiO/SPCE after 0.1 M $K_3[Fe(CN)_6]$ drops is shown in Fig. 5. As a result, the diameter of the semicircle on the NiO/SPCE is larger than that of the bare SPCE. The diameter of the semicircle is the same as the R_{ct} value. The NiO/SPCE sensor has an R_{ct} value of 1276.79 Ω and the bare SPCE has an R_{ct} value of 429.06 Ω. The higher the R_{ct} value, the slower the electron transfer rate in the electrode. Therefore, the electron transfer rate on the NiO/SPCE is slower than that of the bare SPCE.

Another case, Fig. 6a and Fig. 6b show cyclic voltammograms obtained when detected 0.1 M $K_3[Fe(CN)_6]$ with bare SPCE and NiO/SPCE, with an applied voltage ranging from -1 V to 1 V and a scan rate varying from 10 mV/s to 25 mV/s, 50 mV/s, 100 mV/s, and 175 mV/s. When the scan rate is 10 mV/s and 100 mV/s, the NiO/SPCE detects higher anode peak currents (I_{pa}) and cathode peak currents (I_{pc}) than the bare SPCE. Meanwhile, at a scan

rate of 25 mV/s, 50 mV/s, and 175 mV/s, the NiO/SPCE detects smaller I_{pa} and I_{pc} than the bare SPCE. Whether the NiO/SPCE or bare SPCE detects it, the I_p gets higher when the scan rate is increased. After that, the inset of Fig. 6a and Fig. 6b shows the linear regression of Ip with the x-axis as the root of the scanning rate and the y-axis as the current. The gradient value is measured. The larger the gradient value, the more sensitive [18] it is because the current changes when the scanning rate is increased, or the response effect is greater. The I_{pa} gradient value on the NiO/SPCE is bigger, which is 5.17×10^{-3} A√(s/V) than the bare SPCE, which is 4.98×10^{-3} A√(s/V). This indicates that the NiO/SPCE is more sensitive than the bare SPCE during the oxidation reaction. Meanwhile, for Ipc, the NiO/SPCE is smaller, at -4.68×10^{-3} A√(s/V) than the bare SPCE, which is -4.89×10^{-3} A√(s/V). This indicates that the NiO/SPCE is not more sensitive than the bare SPCE during the reduction reaction. Through this gradient value, the surface area of the active electrode is measured based on the Randles-Sevcik equation [19] in Equation (3).

$$I_P = \left(2.678 \times 10^5\right) A C_k n^{3/2} D_k^{1/2} v^{1/2} \tag{3}$$

where Ip is the current (A), v is the scanning rate (V/s), n is the number of electrons involved in the redox equation (mol e^-/mol reactance), A is the surface area of the active electrode (m^2), Dk is the constant diffusion (m^2/s), and Ck is the concentration (mol/m^3). As a result, the active electrode surface area of the NiO/SPCE is 0.071 cm^2 while the bare SPCE is 0.069 cm^2.

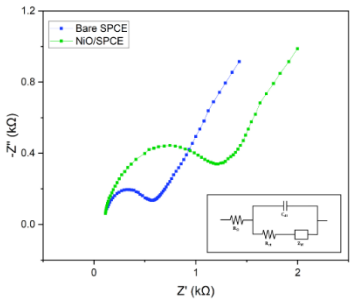

Fig. 5. Nyquist plots of 0.1 M $K_3[Fe(CN)_6]$ at bare SPCE (blue) and NiO/SPCE (green). Inset: Randles Circuit.

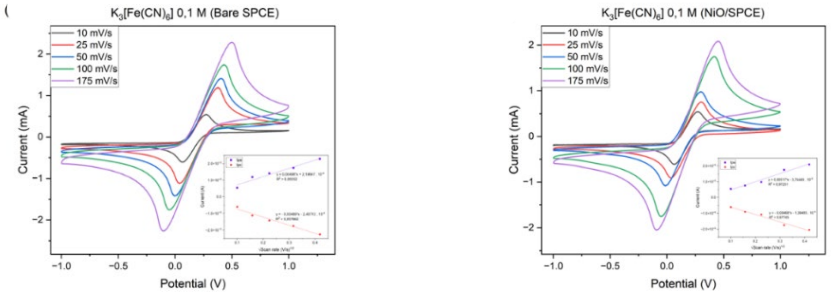

(a) (b)

Fig. 6. Cyclic voltammogram of 0.1 M $K_3[Fe(CN)_6]$ at (a) bare SPCE and (b) NiO/SPCE with scan rate variation (potential applied: -1 V to 1 V). Inset: linear regression from I_{pa} and I_{pc}.

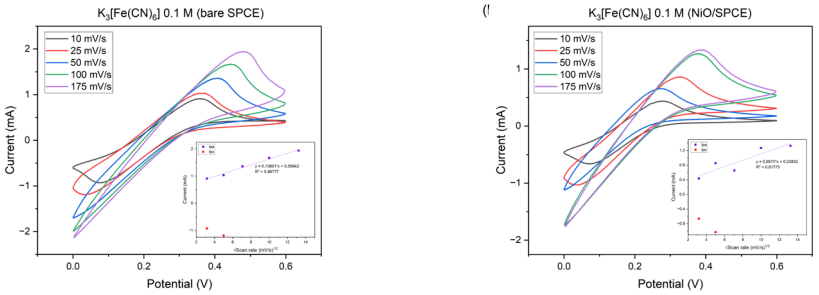

(a) (b)

Fig. 7. Cyclic voltammogram of 0.1 M $K_3[Fe(CN)_6]$ at (a) bare SPCE and (b) NiO/SPCE with scan rate variation (potential applied: 0 V to 0.6 V). Inset: linear regression from I_{pa} and I_{pc}.

3.2 Reference data

The Reference data acquisition was carried out using a commercial potentiostat. In contrast to Fig. 6, which shows cyclic voltammetry when given a voltage of -1 V to 1 V, Fig. 7 shows the cyclic voltammetry produced at voltage of 0 V to 0.6 V. When compared, in the potential range of 0 V to 0.6 V, voltammogram cyclic does not resemble "duck" shape. When the scan rate is 100 mV/s and 175 mV/s, no I_{pc} is detected. The inset in Fig. 7 shows the I_{pa} point with linear regression and the I_{pc} point. The gradient value on the NiO/SPCE is smaller, namely 0.087 A$\sqrt{}$(s/V), compared to 0.107 A$\sqrt{}$(s/V) for the bare SPCE. As a result, the NiO/SPCE is no more sensitive to $K_3[Fe(CN)_6]$ detection than the bare SPCE.

When the glucose concentration was varied, the experiment was carried out three times to obtain the average peak current value, which would be used to calculate the LOD (limit of detection) and LOQ (limit of quantitation) values. LOD is the smallest limit test parameter owned by a tool to measure a certain amount of analyte. Meanwhile, LOQ is the smallest amount of analyte in the sample that can still be measured accurately and with precision by the tool [20]. The LOD and LOQ formulas are shown in Equation (4) and Equation (5).

$$LOD = \frac{k_D \cdot \sigma}{m} \tag{4}$$

$$LOQ = \frac{k_Q \cdot \sigma}{m} \tag{5}$$

where k_D as the multiplication factor which is worth three, k_Q as the multiplication factor which is worth ten, m as the gradient value, and as the standard deviation [19].

Figures 8a, 8b, and 8c show the glucose detection carried out with the bare SPCE the first time, the second time, and the third time in the range of -1 V to 1 V represented by the fifth cycle. Only I_{pc} is visible, and even then it is very low. I_{pc} is processed by linear regression to see the gradient value. The more frequent the experiment, the smaller the gradient value, namely -5.70×10^{-3} mA/mM, -5.14×10^{-3} mA/mM, and -4.95×10^{-3} mA/mM for the first, second, and third trials. This indicates that the more frequent the trials, the less sensitive the bare SPCE. Then, the Ipc from each experiment was taken and averaged based on the concentration as shown in Fig. 8d with a gradient value of -4.04×10^{-3} mA/mM. After processing, the LOD value was 2.629 mM and the LOQ value was 8.762 mM.

Meanwhile, Fig. 9 shows the cyclic voltammogram tested on NiO/SPCE with the same potential range and variation as Fig. 8. The result is the same as when detected with bare

SPCE, only I_{pc} is visible and even then it is low. I_{pc} was processed by linear regression to see the gradient values, namely -7.43×10^{-3} mA/mM, -6.93×10^{-3} mA/mM, and -7.84×10^{-3} mA/mM for the first, second, and third trials. The NIO/SPCE's sensitivity decreased on the second trial and increased again on the third trial. Then, the I_{pc} of each trial was taken and then averaged based on the concentration. Figure 9d depicts the average linear regression of I_{pc} with a gradient value of -7.42×10-3 mA/mM. After that, the LOD value was 1.807 mM and the LOQ value was 6.024 mM.

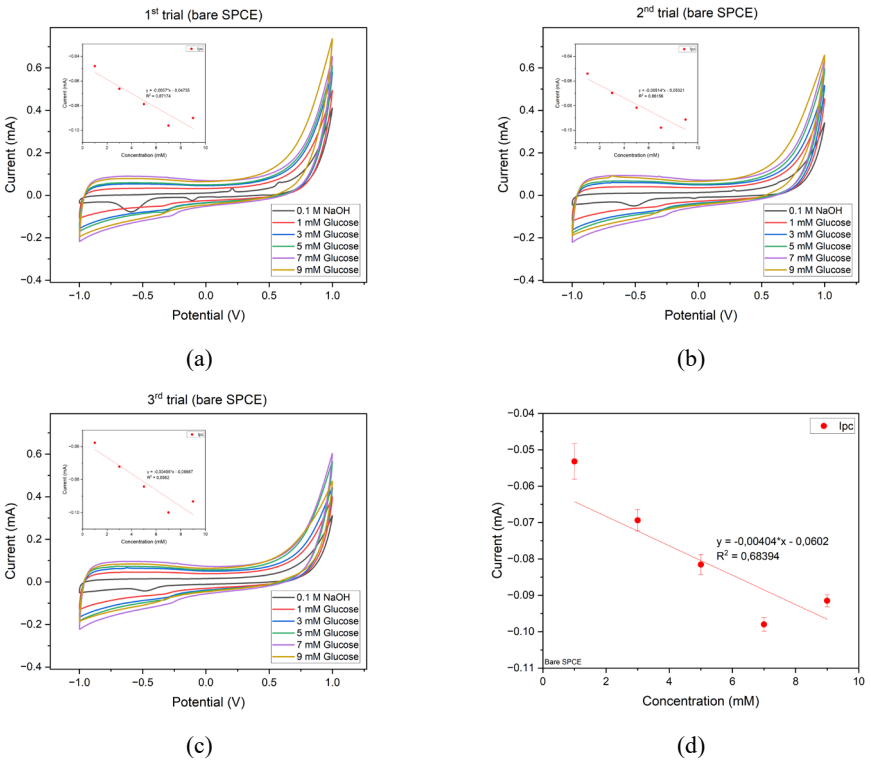

Fig. 8. Cyclic voltammogram when glucose of varying concentration is detected by a bare SPCE in a potential range of -1 V to 1 V [inset: linear regression of Ipc] for (a) first, (b) second, and (c) third trials, and (d) linear regression from the average of the three trials I_{pc}.

The LOD and LOQ values on the NiO/SPCE are smaller than the bare SPCE. That is, the NiO/SPCE is better able to accurately detect lower glucose concentrations than the bare SPCE. Then, the gradient values in Fig. 8d and Fig. 9d are compared, the NiO/SPCE has a gradient value that is greater than the bare SPCE. This shows that, from the average experiment, the NiO/SPCE is more sensitive at detecting glucose than the bare SPCE. Based on these two comparisons, the NiO/SPCE is more suitable for glucose detection than the bare SPCE.

As shown in Fig. 10, the potential range was changed from -1 to 1 V to 0 to 0.6 V. It is seen that in this potential range there is no Ipa and Ipc, meaning that no oxidation-reduction reaction can be observed either using bare SPCE or NiO/SPCE. If observed from Fig. 8 and 9, Ipc was detected when the voltage was -0.2 V to -0.5 V, so that in the range of 0 V to 0.6 V, Ip was not detected. As a result, it could not measure LOD and LOQ. Then, it was observed that the detected current will increase with increasing concentration,

both when the voltage is 0 V to 0.6 V and -1 to 1 V, even though it is not suitable at certain concentrations. This indicates that the concentration is proportional to the current.

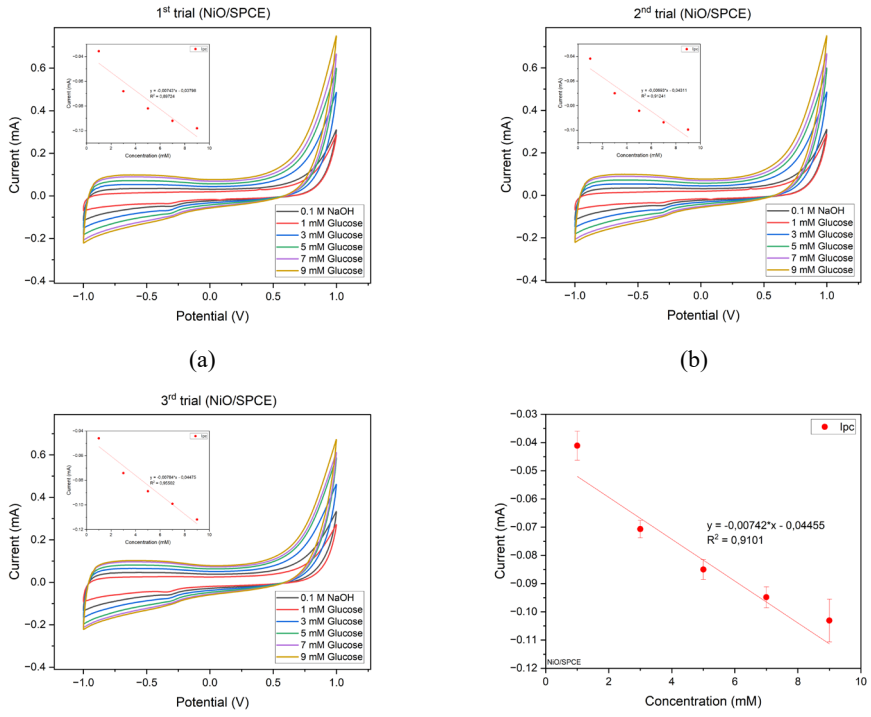

Fig. 9. Cyclic voltammogram when glucose of varying concentration is detected by a NiO/SPCE in a potential range of -1 V to 1 V [inset: linear regression of Ipc] for (a) first, (b) second, and (c) third trials, and (d) linear regression from the average of the three trials I_{pc}.

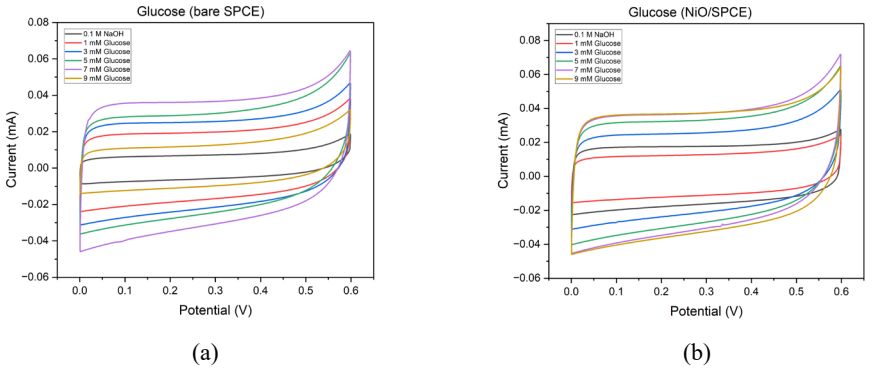

Fig. 10. Cyclic voltammogram when glucose of varying concentrations is detected by (a) bare SPCE and (b) NiO/SPCE in a potential range from 0 V to 0.6 V.

Figure 11 shows a cyclic voltammogram in the fifth cycle of glucose detected by (a) the bare SPCE and (b) the NiO/SPCE based on the variation of the scan rate when a voltage is applied from -1 V to 1 V. Same as when the glucose concentration varies, the cyclic voltammogram is in the potential range from -1 V to 1 V only detects low I_{pc}. The inset in Fig. 11 shows the linear regression of I_{pc}. The gradient value of the NiO/SPCE, which is 8.14×10^{-4} mA s/mV, is smaller than the gradient value of the bare SPCE, which is 9.62×10^{-4} mA s/mV. Therefore, when the scan rate is varied, the NiO/SPCE is not more sensitive than the bare SPCE. The greater the scan rate, the greater the current and I_p detected will be. This indicates that the scan rate is proportional to the current.

After that, the potential range was changed from -1 to 1 V to 0 to 0.6 V as shown in Fig. 12. As with variations in glucose concentration, the cyclic voltammogram in the potential range of 0 to 0.6 V did not detect peak currents either with the bare SPCE or the NiO/SPCE. Then, when the scanning rate is increased, the detected current will be even greater. Then, the NiO/SPCE detects a higher current than the bare SPCE. For example, when the scan rate is 175 mV/s, the NiO/SPCE can detect up to 0.10 mA, while on the bare SPCE it is only up to 0.06 mA.

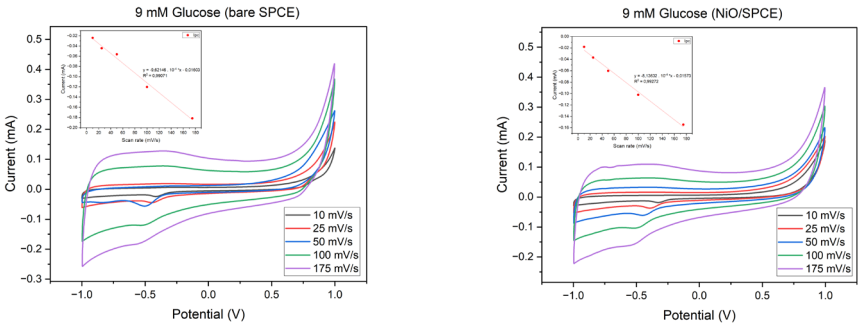

(a) (b)

Fig. 11. Cyclic voltammogram of 9 mM glucose at (a) bare SPCE and (b) NiO/SPCE with scan rate variation (potential applied: -1 V to 1 V). Inset: linear regression from I_{pc}.

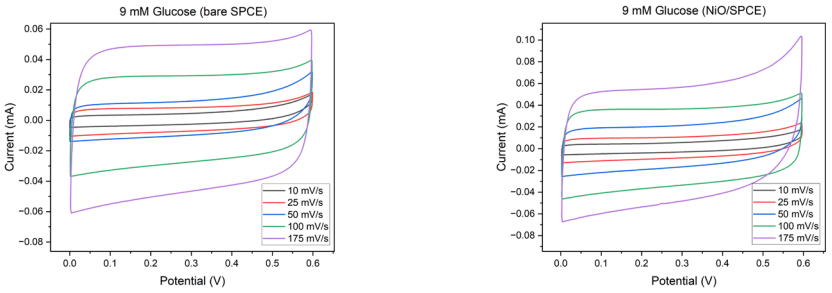

(a) (b)

Fig. 12. Cyclic voltammogram when glucose of varying concentrations is detected by (a) bare SPCE and (b) NiO/SPCE in a potential range from 0 V to 0.6 V.

3.3 Prototype data

The data that has been obtained from the system prototype is processed and compared with the reference data from commercial potentiostats. However, not all reference data can be compared with prototype data because the prototype system can only perform a voltage sweep at a scan rate of 50 mV/s, an applied voltage of 0 to 0.6 V, and one cycle. While on commercial potentiostats, the scan rate, applied voltage, and number of cycles can be varied. Therefore, in the prototype system, five experiments were carried out to represent five cycles as in a commercial potentiostat. Another difference lies in the strengthening of the TIA and the adjustable operating modes of the system prototype. The TIA gain was changed from 2.75 KΩ to 3.5 KΩ to 7 KΩ. Meanwhile, the operating mode used is 3-LEAD AC because the tests carried out involve three electrodes (WE, RE, and CE).

The cyclic voltammograms of the system prototype and a commercial potentiostat (Corrtest) when detecting $K_3[Fe(CN)_6]$ with the bare SPCE and the NiO/SPCE are shown in Fig. 13a and Fig. 13c. The prototype system detects higher currents than commercial potentiostats. Then, the E_{PA} of the NiO/SPCE is the same for the system prototype and commercial potentiostat, which is around 0.25 V. Meanwhile, the E_{PA} of the bare SPCE on the system prototype is about 0.25 V and the commercial potentiostat is around 0.4 V.

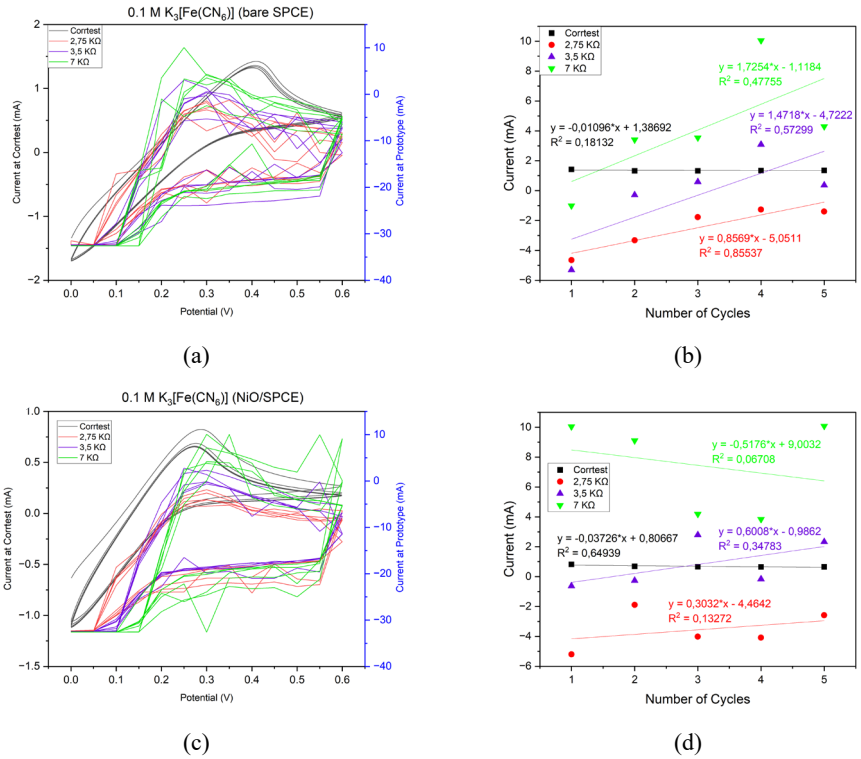

Fig. 13. Cyclic voltammogram of 0.1 M $K_3[Fe(CN)_6]$ when detected (a) bare SPCE with (b) linear regression and (c) NiO/SPCE with (d) linear regression taken on the prototype with TIA gain values (red) 2.75 KΩ, (purple) 3.5 KΩ, and (green) 7 KΩ; and (black) commercial potentiostat.

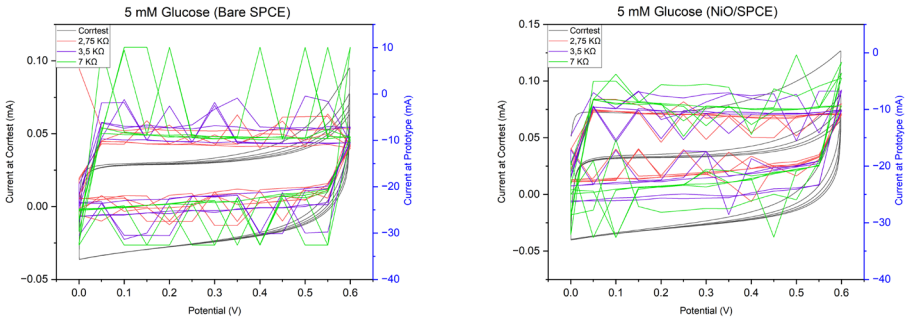

(a) (b)

Fig. 14. Cyclic voltammogram of 5 mM glucose when detected (a) bare SPCE and (b) NiO/SPCE taken on the prototype with TIA gain values (red) 2.75 KΩ, (purple) 3.5 KΩ, and (green) 7 KΩ; and (black) commercial potentiostat..

Then, reviewing the variation of TIA gain from. In the prototype system, it can be seen that the greater the gain given, the more fluctuating the current is obtained. This can be caused because the noise that is being amplified is getting bigger. This statement is reinforced by linear regression in Fig. 14b and 14d. In this case, the gradient value does not indicate the sensitivity of the sensor but shows the stability of the current taken each cycle. Thus, the smaller the detected gradient value, the more stable the current value is taken. The gradient value when TIA gain detected by the bare SPCE is 1.73 mA^{-1}, 1.47 mA^{-1}, 0.86 mA^{-1}, and -1.10×10^{-2} mA^{-1} and the NiO/SPCE is 0.52 mA^{-1}, 0.60 mA^{-1}, 0.30 mA^{-1}, and -0.04 mA^{-1}, respectively for the system prototype at 2.75 KΩ, 3.5 KΩ, and 7 KΩ, and a commercial potentiostat. Thus, it is evident that the greater the gain of TIA, the more volatile the current detected and the most stable commercial potentiostat will be.

Figure 14 shows a comparison of the cyclic voltammogram between the system prototype and a commercial potentiostat (Corrtest) when detecting glucose with the bare SPCE and the NiO/SPCE. In contrast to $K_3[Fe(CN)_6]$, glucose did not detect Ip at all. When the TIA gain value varies, as it does in $K_3[Fe(CN)_6]$, the greater the gain, the more fluctuating the current obtained. If you pay attention to Fig. 13 and 14, the prototype cyclic voltammogram of the system tends to have the same shape as a commercial potentiostat. Although the current obtained by the prototype system is still unstable, insensitive, and noisy when detecting $K_3[Fe(CN)_6]$, it forms I_{pa}. Meanwhile, glucose flat with peak from noise.

4 Conclusion

We have systematically observed dynamics characteristics of SPCE to measure amount of glucose. Sensitivity, LOD and LOQ was observed by impedance method and comparing with cyclic voltammetry. For implementing, transimpedance amplifier has been applied and signal shows relatively influenced by noise caused by connecting problem. By comparing two different SPCE, it was found that NiO/SPCE has better performance than bare SPCE.

Acknowledgements

This work was funded by Hibah Kolaborasi Widya Nano Sensor 2022 - 2023 organized by PT UMG Idea Lab.

References

1. International Diabetes Federation, *Diabetes estimates (20-79 y): People with Diabetes, in 1,000s* (2021), available at https://diabetesatlas.org/data/en/indicators/1/.
2. Rokom, *Pola Hidup Sehat dan Deteksi Dini Bantu Kontrol Gula Darah pada Penderita Diabetes* (2021), available at https://sehatnegeriku.kemkes.go.id/baca/umum/20211115/3438859/pola-hidup-sehat-dan-deteksi-dini-bantu-kontrol-gula-darah-pada-penderita-diabetes/.
3. A. Mandal, *Normal Blood Sugar Values, Molarity and Fluctuations* (2021), available at https://www.news-medical.net/amp/health/Blood-Sugar-Normal-Values.aspx.
4. C. E. Banks C. W. Foster, and R. O. Kadara, *Screen-Printing Electrochemical Architectures* (Spinger, Switzerland, 2016).
5. Drop Sens, *Nickel Oxide modified Screen-Printed Carbon Electrodes*, available at https://www.dropsens.com /en/pdfs_productos/new_brochures/110ni_x1110ni.pdf.
6. J. Zhu et al., Biosens. Bioelectron. **193**, 113606 (2021).
7. A. Debataraja and R.V. M. Hiskia, *Proceeding Conference on Smart-Green Technology in Electrical and Information Systems* (Udayana University Press, 2013), pp. 121–124.
8. P. Busono, R. Febryarto, and M. Mayantasasi, *Pros. Semnastek* (Universitas Muhammadiyah Jakarta, 2018), pp. 1–7.
9. N. Elgrishi et al., J. Chem. Educ. **95**, 197–206 (2018).
10. H. S. Magar, R. Y. A. Hassan, and A. Mulchandani, Sensors **21**, 6578 (2021).
11. A. S. Rajpurohit, N. S. Punde, and A. K. Srivastava, New J. Chem. **43**, no. 42, 16572–16582 (2019).
12. K. Krorakai, S. Klangphukhiew, S. Kulchat, and R. Patramanon, Appl. Sci., **11**, 1–13 (2021).
13. Drop Sens, *Screen-Printed Carbon Electrode*, available at https://www.dropsens.com/en/ pdfs_productos/new_brochures/110-c110.pdf.
14. Texas Instrument, *LMP91000EVM User's Guide* (2012), available at https://www.ti.com/lit/snau121.
15. Raspberry Pi, *Raspberry Pi 3 Model B*, available at https://www.raspberrypi.com/products/raspberry-pi-3-model-b/.
16. Texas Instrument, LMP91000 Sensor AFE System: Configurable AFE Potentiostat for Low-Power Chemical- Sensing Applications (2014), available at https://www.ti.com/lit/gpn/lmp91000.
17. J. Aznar-Poveda, J. A. Lopez-Pastor, A. J. Garcia-Sanchez, J. Garcia-Haro, and T. F. Otero, Sensors **18**, 1–15 (2018).
18. J. Fraden, *Handbook of Modern Sensors* (Springer, Switzerland, 2016).
19. R. M. Granger, H. M. Yochum, J. N. Granger, and K. D. Sienerth, *Instrumental Analysis* (Oxford University Press, Oxford, 2017).
20. D. Sumarno and D. I. Kusumaningtyas, Bul. Teknik Litkayasa Sumber Daya Penangkapan **16**, 7-11 (2018).